

# Automatic Staging and Subtype Determination for Non-Small Cell Lung Carcinoma Using PET Image Texture Analysis

Seyhan Karaçavuş, Bülent Yılmaz, Ömer Kayaaltı, Semra İçer, Arzu Taşdemir, Oğuzhan Ayyıldız, Kübra Eset, Eser Kaya

**Abstract**—In this study, our goal was to perform tumor staging and subtype determination automatically using different texture analysis approaches for a very common cancer type, i.e., non-small cell lung carcinoma (NSCLC). Especially, we introduced a texture analysis approach, called Law's texture filter, to be used in this context for the first time. The 18F-FDG PET images of 42 patients with NSCLC were evaluated. The number of patients for each tumor stage, i.e., I-II, III or IV, was 14. The patients had ~45% adenocarcinoma (ADC) and ~55% squamous cell carcinoma (SqCCs). MATLAB technical computing language was employed in the extraction of 51 features by using first order statistics (FOS), gray-level co-occurrence matrix (GLCM), gray-level run-length matrix (GLRLM), and Laws' texture filters. The feature selection method employed was the sequential forward selection (SFS). Selected textural features were used in the automatic classification by *k*-nearest neighbors (*k*-NN) and support vector machines (SVM). In the automatic classification of tumor stage, the accuracy was approximately 59.5% with *k*-NN classifier (*k*=3) and 69% with SVM (with one versus one paradigm), using 5 features. In the automatic classification of tumor subtype, the accuracy was around 92.7% with SVM one vs. one. Texture analysis of FDG-PET images might be used, in addition to metabolic parameters as an objective tool to assess tumor histopathological characteristics and in automatic classification of tumor stage and subtype.

**Keywords**—Cancer stage, cancer cell type, non-small cell lung carcinoma, PET, texture analysis.

## I. INTRODUCTION

POSITRON emission tomography (PET) is a useful functional imaging technique whose effectiveness to stage or restage tumors, to evaluate tumor response to treatment,

define patient prognosis, and guide surgery and radiotherapy for patients with cancers of non-small cell lung cancer (NSCLC) is proven [1], [2]. The uptake of 18F-FDG used extensively in PET studies is closely related to the parameters determining the biological behavior of the lesion such as in healthy, tumorous, and inflammatory cells, growth index, tissue blood supply, hypoxia [3]. Therefore, a more meaningful feature of the tumor uptake from PET images for the determination of intratumoral heterogeneity has recently been investigated intensively. Texture analysis of PET images may allow us to characterize the histopathological tumor properties in vivo in molecular level. Texture analysis includes a set of pattern analysis approaches that quantify the interrelationship of the pixels or voxels via different mathematical methods. Our goal was to introduce for the first time a texture analysis approach, called Law's texture filter, in the intratumoral heterogeneity quantification for finding features useful in the classification of the tumor stage and subtype for a very common cancer type, i.e., non-small cell lung carcinoma.

## II. METHODS

### A. Patient Population and PET/CT Study

In this retrospective study, 38 patients with non-small cell lung cancer that previously underwent 18F-FDG PET/CT imaging for cancer staging before chemo-radiotherapy treatment were evaluated in Acibadem Hospital, Nuclear Medicine Department, Kayseri, Turkey, using a PET/CT scanner (Siemens Biograph 6, HiRez, Siemens-CTI, Knoxville, TN, USA). The patient population consisted of 4 females and 38 males, with a mean age of 62.4±8.7, were evaluated in this study. In order to balance the group sizes, patients with stage I and 2 were combined to form one group, giving a total of three groups (stages I&II, stage III, and stage IV). The number of patients with each stage was 14. The tumor subtypes were also balanced: Adenosquamous carcinoma (ADC) patients 19 and squamous cell carcinoma (SqCC) patients 23. In order to better determine the biological behavior, and tumor type, the pathological specimens of the patients were re-examined. The slides that best exemplified the tumor were selected and re-evaluated under a light microscope by the expert pathologist in our team.

S. Karaçavuş is with the School of Medicine at Bozok University, Yozgat, Turkey (e-mail: seyhan.karacavus@bozok.edu.tr).

B. Yılmaz and O. Ayyıldız are with the Electrical-Electronics Engineering Department of Abdullah Gül University, Kayseri, Turkey (e-mail: bulent.yilmaz@agu.edu.tr, oguzhan.ayyildiz@agu.edu.tr).

Ö. Kayaaltı is with the Department of Computer Technologies, Develi Hüseyin Şahin Vocational College, Erciyes University, Kayseri, Turkey (e-mail: kayaalti@erciyes.edu.tr).

S. İçer and K. Eset are with the Biomedical Engineering Department, Erciyes University, Kayseri, Turkey (e-mail: ksemra@erciyes.edu.tr, kbra.eset7@gmail.com).

A. Taşdemir is with the Department of Pathology, Kayseri Educational and Research Hospital, Kayseri, Turkey (e-mail: atasdemir@erciyes.edu.tr)

E. Kaya is with the Nuclear Medicine Department of Acibadem Hospital, Kayseri, Turkey (e-mail: kaya\_eser@yahoo.com)

This study is supported by TUBITAK (The Scientific and Technological Research Council of Turkey) under Project No: 118E188.

### B. Image Processing and Texture Analysis

The PET/CT images and acquisition details were saved as DICOM image files. The PET/CT slices that contained tumor lesions were marked and evaluated using the graphical user interface of the acquisition system infused and separate modes. For each patient, 12-20 PET slices that contained tumors were selected for further analysis.

The image processing steps were performed using MATLAB (MathWorks MA, USA) technical computing environment based on the selected slices. The processing steps were as follows: i) tumor segmentation, ii) binning, and iii) texture analysis.

Before the segmentation step, a rectangular region that contained all lesions on the selected slices was visually selected, and *k*-means clustering approach [4] was used to segment the tumor from the background for each slice automatically. The tumorous regions on each slice were concatenated forming a three-dimensional (3D) volume of interest (VOI).

The *k*-means clustering algorithm, as the name implies, is used to separate data into *k* clusters or groups. Let the feature vectors computed from *n* clustered data be  $F = \{f_i \mid i=1,2, \dots, n\}$ . The algorithm initiates *k* cluster centroids  $C = \{c_j \mid j=1,2, \dots, k\}$  by randomly selecting *k* feature vectors using a distance metric, Euclidean distance. The next step is to recompute the cluster centroids based on their group members and then regroup the feature vector according to the new cluster centroids. The clustering procedure stops only when all cluster centroids tend to converge. The number of clusters was 2 in our study. If on a slice an obvious error was visually detected the segmentation was performed again manually.

In the texture analysis approaches, we needed binning of intensity values. In the binning step, the pixel values of the segmented region that contain the tumor were scaled. The binning is done in such way that the wide range of intensity values was linearly mapped to integer values between 1 and 64.

The final step involved performing texture analysis on the binned regions with tumors. A total of 51 features was extracted using first order statistics [5] (FOS, 2 features) and three different texture analysis approaches. The texture analysis approaches were the gray level co-occurrence matrix [6] (GLCM, 4 features), gray level run length matrix [7] (GLRLM, 11 features), and the Laws' texture filters [8] (Laws, 34 features).

In FOS, from the pixel intensity values, a histogram depicting the ratio of the number of pixels with a certain gray level to the total number of pixels in the region was formed. Using the pixel intensity values and the histogram the mean, standard deviation values were computed.

GLCM describes the relationship between the neighbor pixels and depicts the occurrence rate of the brightness levels on the image at fixed distances and orientations. GLCMs were computed for 0, 45, 90, and 135 degrees with one-pixel distance. All the features were computed and averaged over 13 angles to make them rotationally invariant. In this approach,

binned VOIs were used in order to describe or characterize the relationship between the neighbors in a standardized manner.

The other feature extraction approach was the GLRLM. The term gray level run in the GLRLM approach means the sequential pixels with the same gray level in the same direction. GLRLM is a 2-D matrix, and each element shows how many times the gray level *i* runs in length of *j* in the angle  $\alpha$  direction occurred. When the number of neighbor pixels that have the same gray level is low, the texture has a fast variation.

Finally, we used a new approach in this context for the first time. It is referred to as the Laws' filters in which local filters are employed in detecting various types of textures. In order to generate these local filters, one-dimensional kernels known as "Level (L), Edge (E), Spot (S), Wave (W), and Ripple (R)" are convolved to produce two or three-dimensional kernels. In our case, the length of L, E, S, W, and R kernels were 3. These filters are later used in determining the strength or energy of different types of textures. Once a filter is applied to the image, resultant filtered image is further processed by windowing, offset and normalization operations. Finally, from the output of these steps mean and standard deviation are computed and used as the features.

### C. Automatic Classification of Tumor Stage and Subtype

One of the aims of our study was to analyze the feasibility of using pattern classification approaches for the discrimination of three tumor stages (stages I-II, stage III, and stage IV) and tumor subtypes (adenocarcinoma -ADC- and squamous cell carcinoma -SqCC-) with the help of textural features. One of the classification methods we chose was the *k*-nearest neighbors (*k*-NN) approach [9]. We have also investigated the usage of support vector machines (SVM) [10]. In *k*-NN, the samples were multi-dimensional feature vectors each with a tumor stage or subtype label. In the classification phase, a feature vector coming from one VOI was assigned to the class that was most frequently encountered among the *k* nearest samples (*k*=3) using a proper distance metric such as Euclidean distance. Once a training dataset is formed, a test feature vector is classified by assigning it to the class of the most frequently seen neighbors among the *k* training samples nearest to that vector. In SVM, the training samples (features coming from texture analysis approaches) are labeled as a member of one of two (or more) categories/classes. A model, which is a non-probabilistic binary linear classifier, assigns new samples into one class or the other. This model is a depiction of the samples as points in space, mapped so that the samples of the different classes are separated by a well-defined gap that is as wide as possible. Finally, new samples are projected on that same space and estimated to go to a class according to the side of the gap they fall on. In the classification part of our study, there were 3 stage classes or 2 tumor subtype classes. SVM one versus one and one versus all methods were executed with the radial basis function kernel. For both *k*-NN and SVM approaches 3-fold cross-validation (CV) was applied for finding overall prediction accuracy rate.

One of the important steps employed in the classification procedure is called the feature selection in which the best subset representing the original feature set is chosen. For instance, in our study only 5 out of 51 features were selected to be used in the classification phase. We used sequential forward selection (SFS) method as it is easy to implement and it offers reasonable performance [11]. In this method, the 'selected features set' was initiated with an empty set the feature yielding the highest accuracy in the classification of tumor stages was added to the 'selected features set'. Then, other/remaining features were sequentially included in the selected feature set and the combination/set of features yielding the highest performance became the new selected features set and so on. This was continued until five features were selected.

### III. RESULTS

In this section, we will first present an exemplary result from the segmentation part of the study. Fig. 1 shows one lesion in 3D form created from 13 PET slices of one patient.

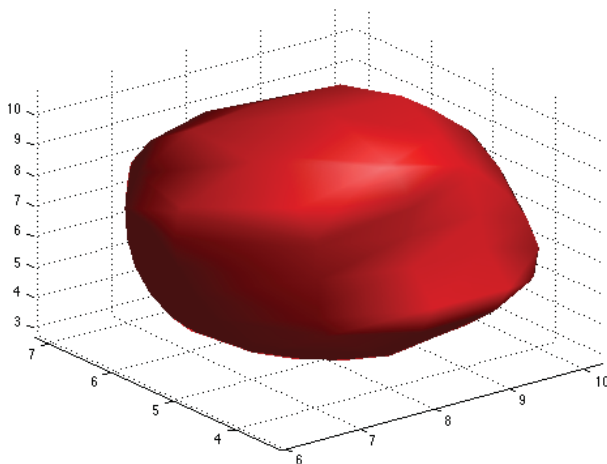


Fig. 1 One tumor in 3D form concatenated from segmented PET slices

#### A. Automatic Tumor Stage Classification

In this part of the study, the classification accuracy of 42 patients was approximately 59.5% with  $k$ -NN classifier ( $k=3$ ) and 69% with SVM (one versus one paradigm), 57% with SVM (one versus all paradigm), using 5 features selected with the SFS method. The increase in the number of features included in the classification phase beyond 5 did not improve the classification accuracy significantly. In this part of the study, with SVM (one vs. one) 3 textural features (Long Run High Gray-Level Emphasis -LRHGE-, Run Percentage -RP-, High Gray-Level Run Emphasis -HGRE-) computed using GLRLM and 2 features (standard deviations of L3S3L3 and S3S3L3) coming from Laws' approach were found to be 5 best features in the classification of three TNM stages.

#### B. Automatic Tumor Subtype Classification

In the classification of tumor subtype there were 19 patients with ADC and 23 patients with SqCC. Out of these 42 patients

the accuracy with  $k$ -NN was 85.7%, with SVM (one vs. one and one vs. all) approach was approximately 92.7%. The selected features, which resulted in the best performance with SVM (one vs. one), were the correlation and energy values of GLCM, Long Run Low Gray-Level Emphasis LRLGE, gray-level non-uniformity (GLN), standard deviation of L3S3S3 computed from Laws' filters.

### IV. DISCUSSION

The 18F-FDG PET is an imaging technique commonly used to study cellular metabolism in oncology. Tumor cells typically show augmented glucose metabolism and thus an increased FDG uptake compared to healthy cells. This characteristic helps the imaging of tumor cells by using PET [12]. In digital PET images, pixels have gray-level intensity values that represent the metabolic rate of glucose corresponding those particular locations/tissues in space [13].

Previous studies have explored the potential use of texture analysis in ultrasonography, computed tomography and magnetic resonance imaging, and reported results supporting the idea that texture features obtained from these images can to differentiate the tissue types [14]-[16]. In recent years, there has been an increased effort to demonstrate the feasibility of texture analysis on PET images, for the evaluation of tumor heterogeneity. The findings of limited number of studies in the literature and our results reveal that certain textural features have more predictive and prognostic power compared to metabolic parameters such as SUVmax or SUVmean.

Some textural features in NSCLC PET images have already been described/used in the literature. For example, Cook et al. evaluated PET textural features in NSCLC and their relationship with response and survival after chemoradiotherapy [17]. In addition, Orhac et al. investigated the correlations between 5 first order statistics and 31 features derived using gray-level co-occurrence matrix, gray-level run length matrix, neighborhood gray-level different matrix, and gray-level zone length matrix approaches [18]. These studies showed that textural features derived from PET images might bring an additional insight into tumor biological behavior.

In this study we used two classification approaches, namely  $k$ -NN and SVM, along with a simple feature selection method, namely sequential forward selection. Here, our aim was to demonstrate the feasibility of using such pattern classification approaches that can scrutinize predictive value of many features simultaneously. Lately, a preliminary study in which the authors have used different texture analysis approaches (not Laws' filters) and linear discriminant analysis (LDA) classification method proposed clustering the tumor subtype in NSCLC [19].

### V. CONCLUSION

Textural features might reflect the biologic abnormalities that underlie disease and have the potential to be used as a new tool to assess tumor metabolism, stage, type and histopathological features in clinical practice in addition to

SUVmax, TLG and MTV. We found that the textural features obtained using Laws' approach along with other commonly used methods could be useful in the discrimination of tumor stage and subtype.

## REFERENCES

- [1] K. Abe, S. Baba, K. Kaneko, Isoda T, Yabuuchi H, Sasaki M, et al. "Diagnostic and prognostic values of FDG-PET in patients with non-small cell lung cancer," *Clin Imag.*, vol. 33, pp. 90-95, 2009.
- [2] Berghmans T, Dusart M, Paesmans M, Hossein-Foucher C, Buvat I, Castaigne C, et al. "Primary tumor standardized uptake value (SUVmax) measured on fluorodeoxyglucose positron emission tomography (FDG-PET) is of prognostic value for survival in non-small cell lung cancer (NSCLC): a systematic review and meta-analysis (MA)," by the European Lung Cancer Working Party for the IASLC Lung Cancer Staging Project. *J Thorac Oncol.*, vol. 3, pp. 6-12, 2008.
- [3] A. Pugachev, S. Ruan, S. Carlin, S.M. Larson, J. Campa, C.C. Ling, et al. "Dependence of FDG uptake on tumor microenvironment," *Int J Radiat Oncol.*, vol. 62, pp. 545-553, 2005.
- [4] J.B. MacQueen, "Some Methods for classification and Analysis of Multivariate Observations," *Proceedings of 5th Berkeley Symposium on Mathematical Statistics and Probability*. University of California Press. pp. 281-297. MR 0214227. Zbl 0214.46201, 1967.
- [5] S. Selvarajah and S. Kodituwakku, "Analysis and comparison of texture features for content based image retrieval," *Int J Latest Trends Computing*, vol. 2(1), pp. 108-113, 2011.
- [6] R.M. Haralic, K. Shanmugan, I.H. Dinstein, "Textural features for image classification," *IEEE Trans Syst Man Cybern Syst.*, vol. SMC-3(6), pp. 610-621, 1973.
- [7] M.M. Galloway, "Texture analysis using gray level run lengths," *Comp Vision Graph.*, vol. 4, pp. 172-179, 1975.
- [8] K.I. Laws, "Textured image segmentation" Ph.D. dissertation, University of Southern California, Los Angeles, CA, 1980.
- [9] N.S. Altman, "An introduction to kernel and nearest-neighbor nonparametric regression," *The American Statistician*, vol. 46 (3), pp. 175-185, 1992.
- [10] C. Cortes and V. Vapnik, "Support-vector networks," *Mach Learn.*, vol. 20, pp. 273-297, 1995.
- [11] A.W. Whitney, "A direct method of nonparametric measurement selection," *IEEE Trans Comput.* vol. 100, pp. 1100-1103, 1971.
- [12] W. Vach, P.F. Høiland-Carlson, O. Gerke and W.A. Weber, "Generating evidence for clinical benefit of PET/CT in diagnosing cancer patients," *J Nucl Med.*, vol. 52, pp. 77-85, 2011.
- [13] G. Castellano, L. Bonilha, L. Li and F. Cendes, "Texture analysis of medical images," *Clin Radiol.*, vol. 59, pp. 1061-1069, 2004.
- [14] K. Holli, A-L. Lääperi, L. Harrison, T. Luukkaala, T. Toivonen, P. Ryymin, et al., "Characterization of breast cancer types by texture analysis of magnetic resonance images," *Acad Radiol.* vol. 17, pp. 135-141, 2010.
- [15] F. Davnall, C.S. Yip, G. Ljungqvist, M. Selmi, F. Ng, B. Sanghera, et al., "Assessment of tumor heterogeneity: an emerging imaging tool for clinical practice?" *Insights Imaging*, vol. 3, pp. 573-589, 2012.
- [16] A. Ba-Ssalamah, D. Muin, R. Scherthaner, C. Kulinna-Cosentini, N. Bastati, J. Stift, et al., "Texture-based classification of different gastric tumors at contrast-enhanced CT," *Eur J Radiol.*, vol. 82, pp. 537-543, 2013.
- [17] G.J. Cook, C. Yip, M. Siddique, V. Goh, S. Chicklore, A. Roy, et al., "Are pretreatment 18F-FDG PET tumor textural features in non-small cell lung cancer associated with response and survival after chemoradiotherapy?" *J Nucl Med.*, vol. 54, pp. 19-26, 2013.
- [18] F. Orlhac, M. Soussan, J-A. Maisonneuve, C.A. Garcia, B. Vanderlinden, I. Buvat, "Tumor texture analysis in 18F-FDG PET: relationships between texture parameters, histogram indices, standardized uptake values, metabolic volumes, and total lesion glycolysis," *J Nucl Med.*, vol. 55, pp. 414-422, 2014.
- [19] S. Ha, H. Choi, G.J. Cheon, K.W. Kang, J-K. Chung, E.E. Kim, et al., "Autoclustering of non-small cell lung carcinoma subtypes on 18F-FDG PET using texture analysis: a preliminary result." *Nucl Med Mol Imaging.*, vol. 48, pp. 278-286, 2014.